




Cite this: *RSC Adv.*, 2025, 15, 22641

# A simple colorimetric sensor based on a new deep eutectic solvent for the detection of chromium†

Thanaporn Seesuan,<sup>a</sup> Nutthaya Butwong,<sup>b</sup> Supalax Srijaranai <sup>a</sup>  
and Siriboon Mukdasai <sup>\*a</sup>

A selective and sensitive method was developed for the detection of  $\text{Cr}^{6+}$ . This method was based on a combination of colorimetry and liquid–liquid extraction using a new deep eutectic solvent (DES). A DES/EDTA (ethylenediaminetetraacetic acid) colorimetric probe was prepared using tetrabutylammonium bromide (TBABr) as a hydrogen-bond acceptor, ascorbic acid (AA) as a hydrogen-bond donor, and EDTA as a chelating agent. Following the reduction of  $\text{Cr}^{6+}$  to  $\text{Cr}^{3+}$  by AA present in the DES/EDTA probe, a purple complex was formed with EDTA, which was immediately extracted into the DES phase. The enriched complex was subsequently quantified by performing absorbance measurements at 550 nm using an ultraviolet-visible spectrophotometer and a smartphone equipped with ImageJ software to detect the color intensity. Under the optimized conditions, the limit of detection was determined to be  $0.056 \mu\text{M}$  ( $2.08 \mu\text{g L}^{-1}$ ) and the linear range was  $0.5\text{--}100 \mu\text{M}$  with a correlation coefficient of 0.9962. In addition, the intra- and inter-day relative standard deviations were  $<6\%$ . Notably, this simple and affordable colorimetric sensor was successfully employed in the detection of chromium in water and soil samples with satisfactory outcomes. The developed approach could therefore be highly useful for the determination of chromium in other environmental and biological samples.

Received 10th April 2025  
Accepted 27th June 2025

DOI: 10.1039/d5ra02492g

rsc.li/rsc-advances

## Introduction

Chromium is useful in a variety of applications, including steel manufacturing, mining, tanning, and electroplating; however, the use of this element can lead to the contamination of underground and surface water resources. In the environment, Cr exists in two stable oxidation states, namely trivalent chromium ( $\text{Cr}^{3+}$ ) and hexavalent chromium ( $\text{Cr}^{6+}$ ). At low concentrations,  $\text{Cr}^{3+}$  is involved in the digestion of proteins, fats, carbohydrates, and nucleic acids,<sup>1</sup> while  $\text{Cr}^{6+}$  is harmful to biological systems, being a suspected carcinogen and mutagen.<sup>2</sup> In addition,  $\text{Cr}^{6+}$  exhibits various short-term and long-term effects, including skin burns, breathing issues, coughing, and wheezing (short-term effects), along with skin, neurological, and gastrointestinal problems (long-term effects).<sup>3,4</sup> Thus, the maximum permissible limit in drinking water is defined by the World Health Organization (WHO) to be  $0.05 \text{ mg L}^{-1}$ .<sup>5</sup>

Conventional methods that are widely employed for chromium detection include flame atomic absorption spectroscopy (FAAS),<sup>6,7</sup> voltammetry,<sup>8</sup> inductively coupled plasma atomic

emission spectroscopy (ICP-AES),<sup>9</sup> inductively coupled plasma mass spectroscopy (ICP-MS),<sup>10</sup> and graphite furnace atomic absorption spectroscopy (GF-AAS).<sup>11</sup> However, these methods are expensive, time-consuming, unsuitable for on-site analysis, and require specialized personnel. Consequently, colorimetric detection methods have been considered for the analysis of heavy metals due to their simplicity, affordability, and capability to produce visible color changes upon interaction with analytes, wherein color changes take place upon complexation of the target metal ions with their specified ligands. Such methods allow facile visualization of the color changes, which vary in intensity depending on the analyte concentration.<sup>12</sup>

Although colorimetric techniques are simple, combining them with pre-concentration methods is typically necessary to enhance detection sensitivity. To date, several techniques have been developed for the pre-concentration and extraction of heavy metal ions from various samples, including solid phase extraction (SPE),<sup>13–15</sup> liquid–liquid extraction (LLE),<sup>16,17</sup> coprecipitation,<sup>18,19</sup> and cloud point extraction (CPE).<sup>20,21</sup> In the context of LLE, there has recently been a shift toward substituting environmentally harmful solvents with alternative solvents that adhere to the principles of green chemistry, including ionic liquids (ILs) and deep eutectic solvents (DESs). ILs consist of organic salts with melting points lower than  $100^\circ\text{C}$ , minimal vapor pressures, low flammability characteristics, and customizable properties. However, their production is

<sup>a</sup>Materials Chemistry Research Center, Department of Chemistry and Center of Excellence for Innovation in Chemistry, Faculty of Science, Khon Kaen University, Khon Kaen 40002, Thailand

<sup>b</sup>Applied Chemistry Department, Faculty of Science and Liberal Arts, Rajamangala University of Isan, Nakhon Ratchasima 30000, Thailand

† Electronic supplementary information (ESI) available. See DOI: <https://doi.org/10.1039/d5ra02492g>



intricate and expensive, and these materials are not biodegradable.<sup>22,23</sup> In contrast, eutectic solvents (ES) are liquid mixtures formed by mixing solid components, wherein a liquid phase is observed when a solid-liquid equilibrium is established. This generates a eutectic system with a significantly reduced melting point. The term “deep” refers to a system wherein the melting point reduction is significantly lower than that of the predicted eutectic temperature when the ideal thermodynamic behavior of the liquid phase is assumed between DES precursors.<sup>24</sup> According to green solvent principles, DESs have been examined as alternative extraction solvents for various industrial applications.<sup>25–27</sup> The growing interest in DESs has arisen from their improved safety and environmental profiles compared to ILs, in addition to their biodegradable nature, low preparation costs, and ease of preparing large solvent quantities for commercial use. Indeed, DESs have been utilized for a wide range of applications including separation processes, solvent extraction, pharmaceutical processing, environmental protection, and materials synthesis.<sup>28,29</sup> Each DES consists of a hydrogen-bond acceptor (HBA), such as a quaternary ammonium or metal salt, and a hydrogen-bond donor (HBD), such as an amine, hydroxyl group, alcohol, or carboxylic acid group.<sup>30–32</sup> DESs can be classified into two types depending on their polarity, namely hydrophobic and hydrophilic DESs.<sup>33</sup> Moreover, hydrophilic DESs decompose in water due to the presence of hydrophilic ammonium, thereby rendering them applicable for use as extraction solvents.<sup>34–36</sup> Recently, an alternative approach integrating DESs with a nylon-based device was reported for Cr detection.<sup>37</sup> This method offered an environmentally friendly solvent system, improved colorimetric stability, and portable analytical capabilities. However, improvements in extraction efficiency are still necessary to enhance its suitability for rapid and simple analysis.

One of the most commonly employed HBA in DESs is tetrabutylammonium bromide (TBABr) because it is low-cost, biodegradable, and non-volatile in nature, in addition to its low toxicity. For analytical purposes, DESs based on TBABr as the HBA have been studied in combination with a variety of HBDs, including formic acid<sup>38</sup> and ascorbic acid (AA).<sup>39</sup>

With the above considerations in mind, the aim of this study is to design a simple and green colorimetric approach for the detection of Cr<sup>6+</sup>. Thus, a liquid colorimetric sensor based on TBABr, AA, and ethylenediaminetetraacetate acid (EDTA) is developed. It is proposed that this sensor is indirectly detect Cr<sup>6+</sup> via its reduction to Cr<sup>3+</sup> by the AA component present in the DES/EDTA probe, followed by subsequent complexation with EDTA to generate a color change from yellow/orange to purple. The resulting complex is enriched in the DES phase, and quantitative analysis is conducted by ultraviolet-visible (UV-vis) spectrophotometry and visual observations using a smartphone equipped with ImageJ software. The proposed technique is applied for the detection of Cr<sup>6+</sup> in environmental water and soil samples, and the results are compared with those obtained using the standard flame atomic absorption spectroscopy (FAAS) method.

## Experimental

### Chemicals and reagents

All solutions were prepared in deionized water (resistivity of 18.2 MΩ cm) that was prepared using a RiOs™ Type I Simplicity 185 system (Millipore, MA, USA). Deionized water was used during all experiments. A stock solution of Cr<sup>6+</sup> was prepared by dissolving analytical grade K<sub>2</sub>Cr<sub>2</sub>O<sub>7</sub> (Ajax Finechem, Auckland, New Zealand) in deionized water. Working standard solutions were freshly prepared from the stock solution *via* stepwise dilutions. Tetrabutylammonium bromide (TBABr) and L-ascorbic acid (AA) were purchased from Sigma-Aldrich (Missouri, USA) and Chem Supply (South Australia, Australia), respectively. Ethylenediaminetetraacetic acid (EDTA) was purchased from APS (Queensland, Australia), while 65 vol% nitric acid was obtained from Sigma-Aldrich (Missouri, USA). The pH values of the solution were adjusted using 0.1 mol L<sup>-1</sup> solutions of sodium acetate and acetic acid (Carlo Erba, Val-de-Reuil, France). Whatman no. 1 filter paper was obtained from GE Healthcare (GE Healthcare, Bangkok, Thailand). All glassware was submerged in 10 vol% nitric acid overnight and washed thoroughly with deionized water prior to use.

### Instrumentation

The UV-vis measurements were performed in the range of 200–800 nm using an Aligent 8453 UV-vis spectrophotometer (Victoria Australia). The Fourier transformed infrared (FT-IR) spectra were recorded using a Bruker Tensor 27 spectrometer. Nuclear magnetic resonance (NMR) spectroscopy was performed for the DESs using a Bruker NMR 400 MHz spectrometer. The zeta potentials of the samples were measured using a Zetasizer nano ZS (Malvern, UK) to confirm the charge on the colorimetric probe. Cyclic voltammetry (CV) was carried out on an AutoLab PGSTAT302N (Utrecht, Switzerland). A three-electrode system was used, which incorporated a 3 mm boron doped diamond electrode (BDD; Windsor Scientific Limited, Berkshire, United Kingdom) as the working electrode, a platinum electrode as the counter electrode (CorrTest, Hebei, China), and Ag/AgCl (3 M KCl) as the reference electrode (CorrTest, Hebei, China).

### Synthesis of the DESs

The DESs were synthesized using TBABr (HBA) and AA (HBD). TBABr and AA were weighed in molar ratios of 1.5 : 1, 2 : 1, and 3 : 1 and heated under magnetic stirring at 300 rpm and 30–40 °C until a homogenous and transparent liquid was formed. The prepared DESs were stored at room temperature until required for use.

### Liquid colorimetric sensor for chromium detection

Fig. 1 outlines the concept of the colorimetric sensor developed herein for the detection of Cr<sup>6+</sup>. To prepare the liquid colorimetric probe (DES/EDTA), a solution of EDTA (500 μL) in acetate buffer (pH 4.0) and THF (500 μL) were added to a centrifuge tube containing DES (500 μL) followed by a Cr<sup>6+</sup> standard or



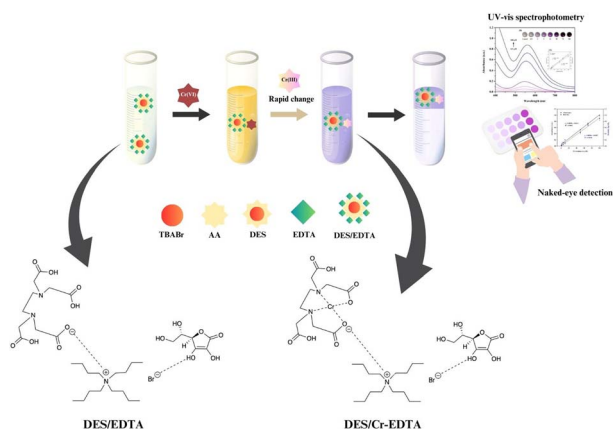


Fig. 1 Schematic diagram of the liquid colorimetric probe used for the detection of chromium.

solution. The solution was then mixed thoroughly by manual shaking. The resulting purple color immediately transferred into the upper layer. The aqueous phase was then removed by syringe, and the enriched phase (DES/Cr-EDTA) was collected for UV-vis absorbance measurements at 550 nm. A photographic image of the enriched phase was recorded using smartphone, and the color intensity (without editing) was evaluated using ImageJ software. Calibration curves were prepared using  $\text{Cr}^{6+}$  at various concentrations, and the red (R), green (G), and blue (B) channels were evaluated. An initial statistical analysis demonstrated that the B channel exhibited a clear linear response with a satisfactory correlation coefficient. The blue (B) channel was therefore selected for the detection of  $\text{Cr}^{6+}$  via a smartphone.

### Sample analysis

The proposed colorimetric sensor was employed for the detection of chromium in environmental water and soil samples, which were collected from Khon Kaen, Thailand. Prior to spiking with  $\text{Cr}^{6+}$ , the water samples were treated with a 1-vol%  $\text{HNO}_3$  solution and passed through filter paper. Extraction of the soil samples (3 mg) was performed using a 1 M HCl solution (20 mL) on a hot plate over 2 h; this procedure was performed in a fume hood. After cooling to room temperature, the solution was filtered through filter paper (Whatman no. 1 filter paper), and the filtrate was collected for analysis.

## Results and discussion

### Characterization of the DES/EDTA probe

The prepared DES was confirmed using a range of techniques, including FT-IR and NMR spectroscopy. The FT-IR spectra recorded for the TBABr, AA, and DES systems are shown in Fig. 2, wherein it can be seen that the DES spectrum contained characteristic peaks corresponding to TBABr (Fig. 2A) and AA (Fig. 2B). Although the FT-IR bands of O–H stretching vibrations are generally observed in the region of  $3200\text{--}2600\text{ cm}^{-1}$ ,<sup>40</sup> it has been reported that the peaks corresponding to O–H stretching

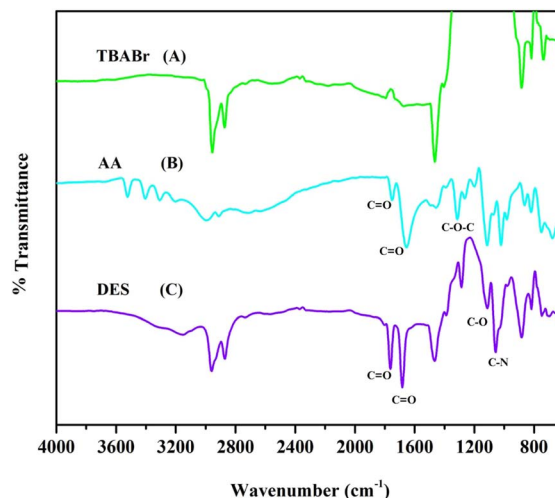


Fig. 2 FT-IR spectra of (A) TBABr, (B) AA, and (C) the DES (TBABr-AA) probe.

vibrations of DESs are related to their structures and can be used to evaluate the presence of hydrogen bonds.<sup>41</sup> Thus, the presence of hydrogen bonding in the prepared DES was confirmed indirectly by comparing the changes in the absorption peak of C=O in the DES and its components because the C=O is closely attached to the O–H group. As shown in Fig. 2C, the absorption peak at  $1682\text{ cm}^{-1}$  assigned as C=O stretching vibration of AA, was shifted to  $1700\text{ cm}^{-1}$  in the DES.<sup>42</sup> In addition, a signal corresponding to the C–O–C stretching vibration of AA can be observed ( $1314\text{ cm}^{-1}$ ), while peaks corresponding to the C–N stretching vibrations of TBABr are present at  $1058$  and  $883\text{ cm}^{-1}$ .

The chemical structure of the DES was then examined using  $^1\text{H}$  NMR spectroscopy (Fig. S1†). All visible peaks were derived from the individual components (TBABr and AA), thereby confirming the purity of the prepared DES. In terms of the physicochemical properties, the melting points of the various DESs were measured (Table S1†), and it was found that the DESs exhibited lower melting points than their components, ultimately confirming their successful synthesis. Furthermore, zeta potential measurements were performed for the fabricated colorimetric probe (DES/EDTA), as listed in Table S2.† The negative zeta potential of the DES ( $-5.05\text{ mV}$ ) became more negative after the addition of EDTA ( $-9.86\text{ mV}$ ), and also after the formation of a complex between  $\text{Cr}^{3+}$  and the EDTA present in the probe ( $-12.7\text{ mV}$ ).

### Fabrication of the colorimetric sensor

The liquid colorimetric sensor was fabricated using the synthesized DES and a ligand. A universal hexadentate ligand, namely EDTA, was chosen because of its low cost, good stability, and high solubility. In addition, the purple complex formed by the combination of  $\text{Cr}^{3+}$  with EDTA in metal-to-ligand ratio of 1 : 1 is known to be stable over a wide pH range,<sup>43</sup> with a high  $\log K_f$  value of 23.40.<sup>44</sup> Notably, the  $\text{Cr}^{3+}$ /EDTA complex generated in the DES has more negative zeta potential ( $-12.7\text{ mV}$ )



than the DES itself and compared to the DES/EDTA probe (Table S2†). The experimental parameters affecting the performance of the fabricated probe were investigated and optimized. All experiments were performed in triplicate using a 20  $\mu\text{M}$   $\text{Cr}^{6+}$  solution, and the absorbance at 550 nm was used to evaluate the efficiency of colorimetric sensor. Moreover, the color intensity attributed to the generated complex was evaluated using a smartphone equipped with ImageJ software.

For comparison, the detection of  $\text{Cr}^{6+}$  was performed both in the presence and absence of EDTA. Following absorbance measurements and detection of the blue intensity, it was found that both the absorbance and the blue intensity were significantly higher in the presence of EDTA (Fig. 3A). It was therefore envisaged that  $\text{Cr}^{6+}$  was reduced to  $\text{Cr}^{3+}$  by the AA present in the DES/EDTA probe, and that it subsequently formed a stable purple-colored complex with EDTA.

The EDTA ( $0.1 \text{ mol L}^{-1}$ ) volume (100–700  $\mu\text{L}$ ) was also examined, and the obtained results indicated that the absorbance increased significantly with an increase in the EDTA volume from 100 to 500  $\mu\text{L}$ , prior to subsequently decreasing at

higher volumes (Fig. 3B). The trend in the blue intensity was similar to that of the absorbance, indicating that the optimal EDTA volume for  $\text{Cr}^{6+}$  detection was 500  $\mu\text{L}$ ; this volume was employed in subsequent experiments.

### Optimization of the DES composition

Using TBABr as an ionic HBA due to its abundance and cost-effective nature, a range of HBDs were investigated, including citric acid (CA), malonic acid (MA), and AA. Following preparation of the liquid probes using the obtained DESs, it was found that the highest absorbance intensity was achieved using the TBABr/AA system (Fig. 4A), thus, AA was selected as the HBD.

Cyclic voltammetry was performed to investigate the reaction of  $\text{Cr}^{6+}$ , and the corresponding results are shown in Fig. S2.† The anodic ( $E_{\text{pa}}$ ) peak potential was observed at +1.35 V,<sup>45</sup> corresponding to the oxidation reaction of  $\text{Cr}^{6+}$  (Fig. S2b†). After the addition of AA (0.01 mol) to the  $\text{Cr}^{6+}$  solution, the peak current of  $\text{Cr}^{6+}$  in the presence of AA decreased compared with that of  $\text{Cr}^{6+}$  in the absence of a reductant and obtained a peak potential at +1.26 V as  $\text{Cr}^{3+}$ <sup>45</sup> (Fig. S2d†). In addition, the oxidation peak of AA showed at +0.70 V<sup>45</sup> (Fig. S2c†). These results indicated that  $\text{Cr}^{6+}$  was completely reduced to  $\text{Cr}^{3+}$  by AA.

The influence of the DES composition on the  $\text{Cr}^{6+}$  detection efficiency was also examined using different TBABr/AA molar ratios (*i.e.*, 1.5 : 1 to 3 : 1), as presented in Fig. 4B. At a ratio of 1.5 : 1, the solvent was slightly viscous, rendering it unsuitable for use. Based on the absorbance values and blue intensities, a molar ratio of 2 : 1 was selected as optimal for the DES/EDTA probe.

Quantitative analysis using UV-vis spectrophotometry requires a sufficient volume of the extraction solvent. Consequently, the effect of the DES volume was examined between 300 and 1000  $\mu\text{L}$ . As illustrated in Fig. 4C, the absorbance signal and blue color intensities increased as the DES volume was increased to 500  $\mu\text{L}$ , but slightly decreased upon increasing the volume to 700 and 1000  $\mu\text{L}$ , likely due to the dilution effect. These results were confirmed by examination of the photographic images. Consequently, a DES volume of 500  $\mu\text{L}$  was selected for subsequent experiments. Considering that aprotic solvents are miscible in both organic and aqueous phases,<sup>46</sup> a selection of solvents were investigated to enhance the phase separation performance. Evaluations using acetone, acetonitrile, and tetrahydrofuran (THF) showed that phase separation of the purple Cr-enriched phase was rapid achieved upon the addition of THF (Fig. S3A, S3B and Table S3†).

### Effect of pH

In such systems, the pH of the aqueous solution plays a key role in defining the forms adopted by the chelating agent, the extent of complex formation, and the resulting extraction efficiency. The effect of pH on complex formation between Cr and EDTA was therefore investigated in a  $0.1 \text{ mol L}^{-1}$  acetic acid/acetate buffer at pH values between 3.0 and 6.0. As illustrated in Fig. 4D, low absorbance and blue intensities were observed at pH 3.0 due to the generation of an unstable complex with a low formation constant.<sup>47</sup> The highest absorbance and blue

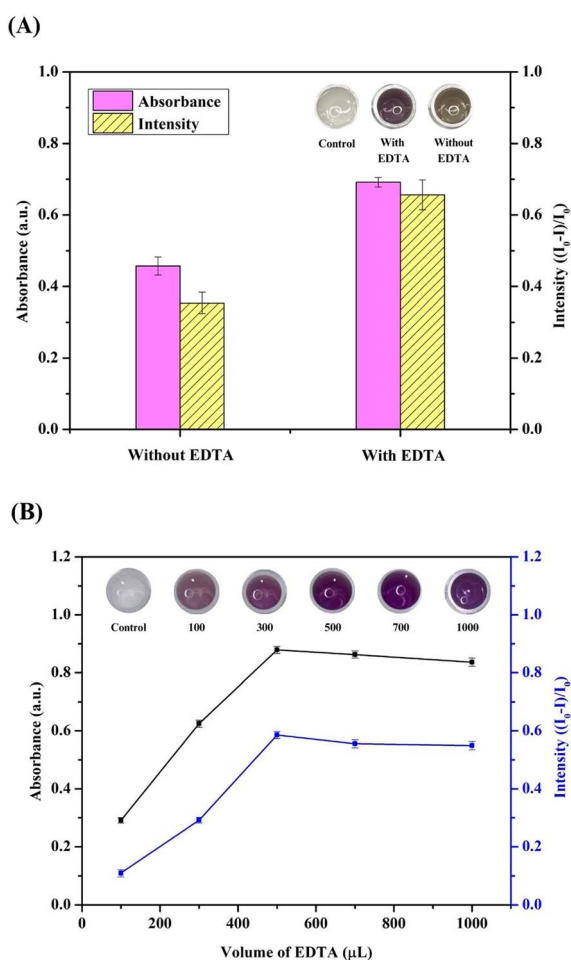


Fig. 3 Effects of EDTA on Cr detection: (A) Cr detection in the presence and absence of EDTA, and (B) effect of the EDTA ( $0.1 \text{ mol L}^{-1}$ ) volume. Extraction conditions: 20  $\mu\text{M}$   $\text{Cr}^{6+}$ ,  $0.1 \text{ mol L}^{-1}$  acetate buffer (pH 4.0), TBABr/AA ratio = 2 : 1, and DES volume = 500  $\mu\text{L}$ .



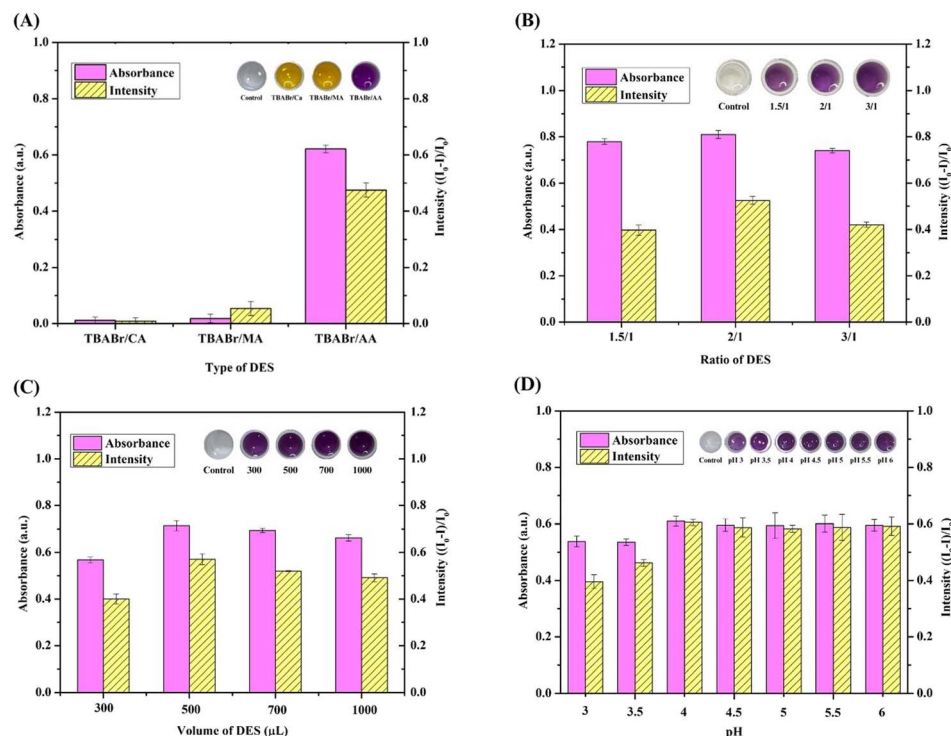


Fig. 4 Optimization of the colorimetric sensor: (A) effect of the DES type. Extraction conditions:  $20\ \mu\text{M}\ \text{Cr}^{6+}$ ,  $0.1\ \text{mol L}^{-1}$  acetate buffer (pH 4.0), 2 : 1 DES ratio, and 500  $\mu\text{L}$  DES. (B) Effect of the DES ratio. Extraction conditions:  $20\ \mu\text{M}\ \text{Cr}^{6+}$ ,  $0.1\ \text{mol L}^{-1}$  acetate buffer (pH 4.0), TBABr/AA DES, and 500  $\mu\text{L}$  DES. (C) Effect of the DES volume. Extraction conditions:  $20\ \mu\text{M}\ \text{Cr}^{6+}$ ,  $0.1\ \text{mol L}^{-1}$  acetate buffer (pH 4.0), DES/EDTA probe. (D) Effect of the solution pH. Extraction conditions:  $20\ \mu\text{M}\ \text{Cr}^{6+}$ ,  $0.1\ \text{mol L}^{-1}$  acetate buffer, 500  $\mu\text{L}$  DES/EDTA probe.

intensity were obtained at pH 4.0; beyond this point, no improvements were observed, thus acetate buffer at pH 4.0 was selected as optimal for the current system.

### Selectivity of the colorimetric sensor for chromium detection

Generally, the colorimetric analysis of metal ions is based on a high selectivity between the metal ions and specific ligands. To evaluate the selectivity of the proposed system, the effects of other potentially interfering ions present in environmental water and soil samples were also investigated. More specifically, these investigations were performed using individual ions at a concentration of  $20\ \mu\text{M}$ , and binary mixtures containing  $20\ \mu\text{M}$  of  $\text{Cr}^{6+}$  and  $20\ \mu\text{M}$  of the interfering ion. As illustrated in Fig. 5A, the purple color was only observed in the presence of  $\text{Cr}^{6+}$ , thereby confirming the selectivity of the probe. Although it can be seen from Fig. 5B that purple solutions were formed in the presence of all interfering ions, no significant differences in absorbance were observed between the various solutions. Although a slightly lower absorbance was observed in the presence of  $\text{Pb}^{2+}$ , this difference was  $<10\%$ , which is considered acceptable due to the hard and soft acids and bases (HSAB) principle.<sup>48</sup> These results therefore confirm the excellent selectivity of the proposed colorimetric sensor for the detection of  $\text{Cr}^{6+}$ .

### Sensitivity of the proposed colorimetric sensor

Subsequently, the performance parameters, including the linear range, limit of detection (LOD), limit of quantification

(LOQ), and precision (intra-day and inter-day), were evaluated under the optimized experimental conditions using UV-vis and a smartphone. The sensitivity of the proposed liquid colorimetric probe was investigated in the presence of various concentrations of  $\text{Cr}^{6+}$ , as shown in Fig. 6 ( $\lambda_{\text{max}} = 550\ \text{nm}$ ). An excellent linearity was observed in the concentration range of  $0.5\text{--}100\ \mu\text{M}$ , giving a regression equation of  $y = 0.0090x + 0.0507$  (Fig. 6A), and a correlation coefficient ( $R^2$ ) of 0.9926. Moreover, the effect of the Cr concentration and the blue intensity was estimated using photographic imaging combined with ImageJ software (Fig. 6B and C). A curve was plotted between the change in blue intensity ( $I_0 - I/I_0$ ) and the Cr concentration, where  $I$  and  $I_0$  are the blue intensity of the resulting complex and blue intensity of the blank solution, respectively, giving  $y = 0.0096x + 0.0507$  and  $R^2 = 0.9962$ . The limit of detection (LOD) and limit of quantitation (LOQ) were calculated based on  $3\sigma/S$  and  $10\sigma/S$ , respectively, where  $\sigma$  is the standard deviation of the response and  $S$  is the slope of the calibration curve. Consequently, the LOD and LOQ values were calculated to be 2.08 and  $7.07\ \mu\text{g L}^{-1}$ , respectively. The precision of the colorimetric probe was expressed as the relative standard deviation in percentage (% RSD,  $n = 5$ ) when measuring  $20\ \mu\text{M}\ \text{Cr}^{6+}$  in one (intra-day) and five consecutive days (inter-day). The results indicate that the proposed probe has good precision with % RSD values less than 6.0%. Additionally, the performance of the proposed colorimetric probe for the determination of chromium was compared with previously reported probes based on colorimetric sensors, as summarized in Table 1. The obtained



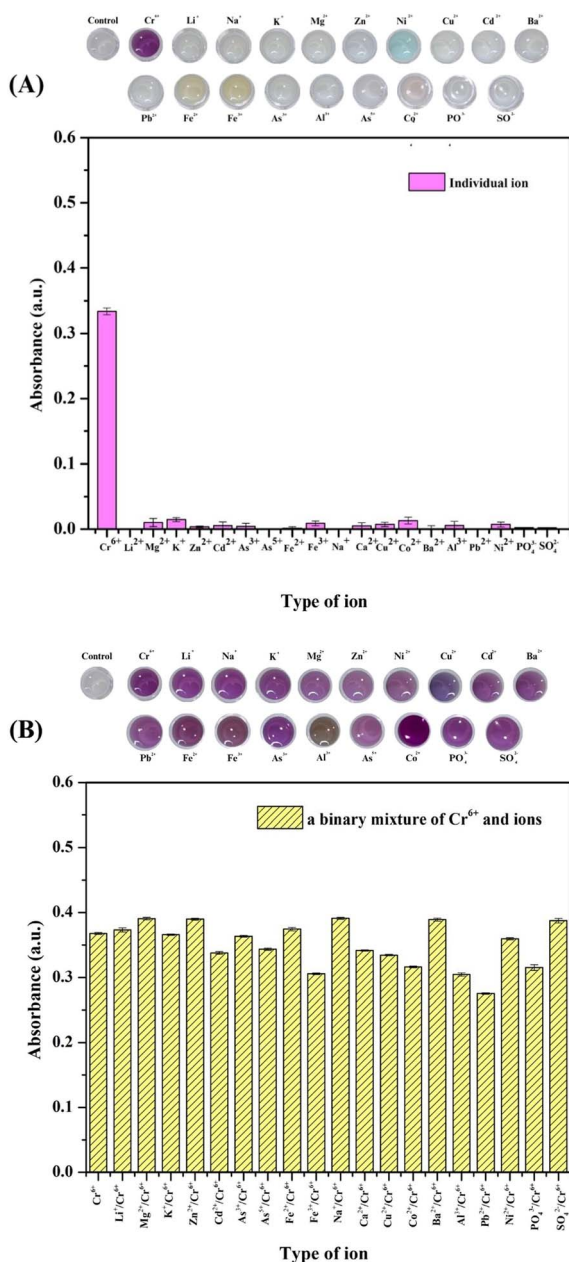


Fig. 5 Selectivity of the colorimetric sensor: (A) relative changes in the absorption intensity of the DES/EDTA system in the presence of different individual ions (20  $\mu\text{M}$ ). (B) Relative changes in the absorption intensity of the DES/EDTA system in the presence of a mixture containing  $\text{Cr}^{6+}$  (20  $\mu\text{M}$ ) and individual interfering ions (40  $\mu\text{M}$ ). Photographic images of the corresponding solutions are also shown.

results clearly indicate that this newly developed colorimetric sensor is more sensitive than previously reported systems. Moreover, the proposed colorimetric method is superior to alternative techniques due to its simplicity and environmental friendliness. Notably, this is the first study to employ the DES/EDTA combination as a liquid colorimetric sensor for  $\text{Cr}^{6+}$  detection.

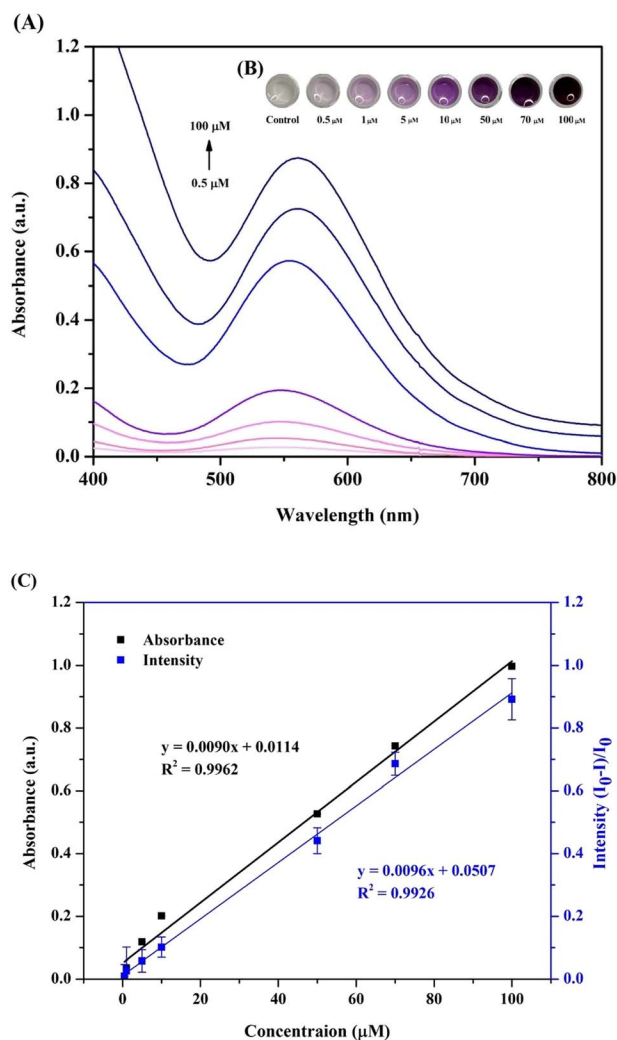


Fig. 6 Quantitative study of the colorimetric sensor for  $\text{Cr}^{6+}$  detection: (A) effect of the Cr concentration on the absorbance intensity (control = DES). (B) Photographic images for the corresponding solutions of panel (A). (C) Calibration plots obtained by plotting the absorbance intensity and the blue intensity  $(I_0 - I)/I_0$  against the  $\text{Cr}^{6+}$  concentration.

### Detection of chromium in real sample

To verify the applicability of the proposed sensor, it was applied for the detection of  $\text{Cr}^{6+}$  in environmental water and soil samples. To compensate for the matrix effect, matrix-matched calibration curves plotted using seven different Cr concentrations were employed. Notably,  $\text{Cr}^{6+}$  was not detected in all the studied samples. The accuracy of the proposed methodology was then studied in terms of the percentage recovery, where in known amounts of  $\text{Cr}^{6+}$  (20, 50, and 70  $\mu\text{M}$ ) were spiked into the sample before analysis. As presented in Table 2, acceptable recoveries in the range of 90.8–109.2% were obtained, indicating the potential of this approach for detecting  $\text{Cr}^{6+}$  in real samples. Furthermore, the *t*-test was performed to evaluate any significant differences between the results obtained using the proposed methodology and the FAAS approach (Table S4<sup>†</sup>), based on a *p*-value of 0.05 (at the 95% confidence limit). The

**Table 1** Comparison of the proposed colorimetric sensor for the determination of chromium

Probe	Ligand	LOD ( $\mu\text{g L}^{-1}$ )	Sample	Detection method	Ref.
ChCl/Phenol	DDTC	5.5	Water	FAAS	49
Acetone/[C <sub>8</sub> MIM] [PF <sub>6</sub> ]	IICDET	5.4	Blood	ETAAS	50
1-Undecanol/ethanol	DDTC	3.1	Drinking water	LIBS	51
DES (TBABr/AA)	EDTA	2.08	Water and soil	UV-vis and smartphone	This work

**Table 2** Determination of chromium in environmental water and soil samples

Sample	Spiked ( $\mu\text{M}$ )	Proposed method		
		Found ( $\mu\text{M}$ )	Recovery (%)	RSD (%)
Water 1	0.0	—	—	—
	20.0	20.3	101.8	6.2
	50.0	48.5	97.1	9.9
	70.0	70.3	100.4	6.1
Water 2	0.0	—	—	—
	20.0	21.7	108.7	3.6
	50.0	45.7	91.9	5.3
	70.0	72.7	103.9	6.4
Water 3	0.0	—	—	—
	20.0	20.0	99.9	6.0
	50.0	49.3	98.6	5.9
	70.0	69.7	99.5	4.0
Water 4	0.0	—	—	—
	20.0	20.2	101.0	9.0
	50.0	49.1	98.3	3.0
	70.0	70.1	100.2	5.6
Soil 1	0.0	—	—	—
	20.0	21.8	109.2	6.3
	50.0	45.4	90.8	9.6
	70.0	72.8	104.0	3.6
Soil 2	0.0	—	—	—
	20.0	21.2	106.1	8.4
	50.0	47.6	95.1	2.5
	70.0	72.1	103.0	3.1
Soil 3	0.0	—	—	—
	20.0	21.2	105.9	5.8
	50.0	47.3	94.6	2.1
	70.0	71.9	102.7	5.0

calculated  $t$  value ( $t$ -cal, 1.725) was found to be lower than the tabulated  $t$  value ( $t$ -table, 2.086), indicating that there was no significant difference between the proposed system and the FAAS method.

## Conclusions

This is the first study on the simultaneous colorimetry and LLE for the indirect detection of  $\text{Cr}^{6+}$  using DES. A new DES of TBABr and AA was prepared and used in combination with EDTA, provided DES/EDTA probe which is a simple and green method. The liquid colorimetric (DES/EDTA) probe plays an important role for both detection and preconcentration of  $\text{Cr}^{6+}$ .  $\text{Cr}^{6+}$  was firstly reduced to  $\text{Cr}^{3+}$  by AA, then formed complex with EDTA and instantaneously solvent extracted by DES. Advantages of the

proposed method are simple, highly selective and sensitive. Moreover, the purple-colored complex can be visual detected and quantified using a smartphone equipped with ImageJ software. Consequently, the color change taking place could be easily evaluated for the selective determination of  $\text{Cr}^{6+}$ , even in the presence of potentially interfering metal ions. Furthermore, this sensor was considered to be user-friendly, rapid, and low-cost, in addition to meeting the requirements of green chemistry. It is expected that the described approach will be applicable in indirect method for the determination of  $\text{Cr}^{6+}$  in other environmental and biological samples.

## Abbreviations

ChCl	choline chloride
[C <sub>8</sub> MIM]	1-octyl-3-methylimidazolium
[PF <sub>6</sub> ]	hexafluorophosphate
TBABr/AA	tetrabutylammonium bromide/ascorbic acid
FAAS	flame atomic absorption spectrometry
ETAAS	electro thermal atomic absorption spectrometry
LIBS	laser-induced breakdown spectrometry

## Data availability

The data supporting this article have been included within this article and the ESI.†

## Author contributions

T. S. conceptualization, methodology, writing – original draft; N. B. investigation, visualization; S. S. supervision; S. M. conceptualization, supervision, writing – review and editing.

## Conflicts of interest

There are no conflicts to declare.

## Acknowledgements

Financial supports from Materials Chemistry Research Center (MCRC) and the Center of Excellence for Innovation in Chemistry (PERCH-CIC), Ministry of Higher Education, Science, Research and Innovative, Thailand are gratefully acknowledged. S. Mukdasai also would like to acknowledge the fund supported by Research and Graduate Studies, Khon Kaen University (Research Program, grant number RP67-9-002).

## References

- 1 C. M. Davis, K. H. Sumrall and J. B. Vincent, *Biochemistry*, 1996, **35**, 12963.
- 2 J. A. Jacobs and S. M. Testa, *Chromium (VI) Handbook*, CRC Press, Boca Raton, FL, 2005, pp. 1–22.
- 3 F. Wang, L. Wang, X. Chen and J. Yoon, *Chem. Soc. Rev.*, 2014, **43**, 4312–4324.
- 4 P. Joshi, S. Sarkar, S. Soni and D. Kumar, *Polyhedron*, 2016, **120**, 142–149.
- 5 World Health Organization, *Chromium, Environmental Health Criteria*, 61, Geneva, Switzerland, 1988.
- 6 U.S. Department of Health and Human Services, *Registry of Toxicology Information Program*, National Library of Medicine, Bethesda, MD, 1993.
- 7 M. D. Farahan and F. Shemirani, Supported hydrophobic ionic liquid on magnetic nanoparticles as a new sorbent for preparation and preconcentration of lead and cadmium in milk and water samples, *Microchim. Acta*, 2012, **179**, 219–226.
- 8 E. Cigdem, F. Senkal and M. Yaman, *Food Chem.*, 2013, **137**, 55–61.
- 9 K. Oktor, S. Yilmaz, G. Turker and E. Erkus, *Environ. Monit. Assess.*, 2008, **141**, 97–103.
- 10 D. C. Prabhakara, Y. Riotte, Y. Sivry and S. Subramanian, *Electroanalysis*, 2017, **29**, 1222–1231.
- 11 J. J. Thompson and R. S. Houk, *Anal. Chem.*, 1958, **58**, 2541–2548.
- 12 N. J. Miller-Ihli and J. Food, *Compos. Anal.*, 1996, **9**, 290–300.
- 13 J. W. Lim, T. Y. Kim and M. A. Woo, *Biosens. Bioelectron.*, 2021, **183**, 113228.
- 14 Md. I. Hoque, D. A. Chowdhury, R. Holze, A. N. Chowdhury and M. S. Azam, *J. Environ. Chem. Eng.*, 2015, **3**, 831–842.
- 15 M. A. Habila, Z. A. AlOthman, A. M. El-Toni, J. P. Labis and M. Soylak, *Talanta*, 2016, **154**, 539–547.
- 16 Z. Wei, S. Sandron, A. T. Townsend, P. N. Nesterenko and B. Paull, *Talanta*, 2015, **135**, 155–162.
- 17 A. N. Anthemidis, D. G. Themelis and J. A. Stratis, *Talanta*, 2001, **54**, 37–43.
- 18 P. L. Malvanker and V. M. Shimde, *Analyst*, 1991, **116**, 1081–1084.
- 19 E. Balladares, O. Jerez, F. Parada, L. Baltierra, C. Hernandez, E. Araneda and V. Parra, *Miner. Eng.*, 2018, **122**, 111–129.
- 20 Y. Zh. Peng, Y. M. Huang, D. X. Yuan, Y. Li and Zh. B. Gong, *Chin. J. Anal. Chem.*, 2012, **40**, 877–882.
- 21 Y. Surme, I. Narin, M. Soylak, H. Yuruk and M. Dogan, *Microchim. Acta*, 2007, **157**, 193–199.
- 22 F. Shemirani, K. R. Rahnema and Y. Assadi, *Microchim. Acta*, 2007, **157**, 81–85.
- 23 J. Soares da S Burato, D. A. Vargas Medina, A. L. de Toffoli and E. Vasconcelos Soares Macial, *J. Sep. Sci.*, 2020, **43**, 25–202.
- 24 Y. Chen, Z. Guo, X. Wang and C. Qiu C, Sample preparation, *J. Chromatogr. A*, 2008, **1184**, 191–219.
- 25 E. N. Gilmore, E. N. McCount, F. Connolly, P. Nockemann, M. Swadzba-Kwasny and J. D. Holbrey, *ACS Sustain. Chem. Eng.*, 2018, **6**, 17323–17332.
- 26 A. Shishov, E. N. Gorbunov, L. Moskv and A. Bulatov, *J. Mol. Liq.*, 2020, **301**, 112380.
- 27 A. Shishov, P. Terno, L. Moskv and A. Bulatov, *Talanta*, 2020, **206**, 120209.
- 28 C. Florindo, L. Romero, I. Rintoul, L. C. Branco and I. M. Marrucho, *ACS Sustain. Chem. Eng.*, 2018, **6**, 3888–3895.
- 29 J. Ling, Y. Chan, J. Nandong, S. Chin and K. Ho, *LWT*, 2020, **133**, 110096.
- 30 M. Deetlefs and K. R. Seddon, *Green Chem.*, 2010, **12**, 17–30.
- 31 A. P. Abbot, G. Capper, D. L. Davids, R. K. Rasheed and V. Tambyrajah, *Chem. Comm.*, 2003, **1**, 70–71.
- 32 J. Cao and E. Su, *J. Cleaner Prod.*, 2021, **314**, 127965.
- 33 L. Tome, V. Baiao, W. Silva and C. Brett, *Appl. Mater. Today*, 2018, **10**, 30–50.
- 34 E. Smith, P. Abbott and K. Ryder, *ACS*, 2014, **114**, 10697–11130.
- 35 A. Prabhune and R. Dey, *J. Mol. Liq.*, 2023, **379**, 121676.
- 36 D. Yu, Z. Xue and T. Mu, *Chem. Soc. Rev.*, 2021, **50**(15), 8596–8638.
- 37 S. Chumkong, W. Sapyen, A. Imyim and N. Bhawawet, *Microchem. J.*, 2025, **212**, 113266.
- 38 W. Tang, Y. An and K. H. Row, *TrAC, Trends Anal. Chem.*, 2021, **136**, 116187.
- 39 J. Cao and E. Su, *J. Cleaner Prod.*, 2021, **314**, 127965.
- 40 S. Ali, Z. Zuhra, Q. Han, M. Ahmad and Z. Wang, *Chemosphere*, 2021, **284**, 131305.
- 41 M. Lucarni, Z. Durazzo, S. Pulgar, P. Gabrielli and G. Lombardi-Boccia, *Food Chem.*, 2012, **267**, 223–230.
- 42 T. Li, Z. Song, Y. Dong, J. Shi and J. Fan, *J. Chromatogr. A*, 2020, **1621**, 461087.
- 43 A. Shishov, R. Chroma, C. Vakh, J. Kuchar, A. Simon, V. Andruch and A. Bulatov, *Anal. Chim. Acta*, 2019, **1065**, 49–55.
- 44 J. Wang, Y. Chen, T. Sun, A. Saleem and C. Wang, *Ecotoxicol. Environ. Saf.*, 2021, **209**, 111858.
- 45 J. Cerar, *Acta Chim. Slov.*, 2015, **62**, 538–545.
- 46 X. R. Xu, H. B. Li, X. Y. Li and J. D. Gu, *Chemosphere*, 2004, **57**, 609–613.
- 47 N. Unceta, F. Seby, J. Malherbe and O. F. X. Donard, *Anal. Bioanal. Chem.*, 2010, **397**, 1097–1111.
- 48 S. Ali, Z. Zuhra, Q. Han, M. Ahmad and Z. Wang, *Chemosphere*, 2021, **284**, 131305.
- 49 E. Yilmaz and M. Soylak, *Talanta*, 2016, **160**, 680–685.
- 50 H. Shirkhanloo, M. Ghazaghi and M. Eskandari, *Anal. Chem. Res.*, 2016, **10**, 18–27.
- 51 I. Gaubeur, M. Aguirre, N. Kovachev, M. Hidalgo and A. Canals, *J. Anal. At. Spectrom.*, 2015, **30**, 2541.

